NeuroImage: Clinical 37 (2023) 103347

Contents lists available at ScienceDirect

NeuroImage: Clinical

journal homepage: www.elsevier.com/locate/ynicl

Longitudinal DAT changes measured with [^{18}F]FE-PE2I PET in patients with Parkinson's disease; a validation study

V.S. Kerstens [a,*], P. Fazio [a], M. Sundgren [b], J. Brumberg [a], C. Halldin [a], P. Svenningsson [b], A. Varrone [a]

[a] Department of Clinical Neuroscience, Centre for Psychiatry Research, Karolinska Institutet and Stockholm Health Care Services, Stockholm, Sweden
[b] Karolinska University Hospital, Neuro Department, Stockholm, Sweden

ARTICLE INFO

Keywords:
Dopamine transporter
Parkinson's disease
Positron emission tomography
Longitudinal
Biomarker

ABSTRACT

Background: Dopamine transporter (DAT) PET provides higher resolution than DAT SPECT and opportunity for integrated imaging with MRI. The radioligand [^{18}F]FE-PE2I is highly selective for the DAT, and PET measurements with this radioligand have good reliability and repeatability in patients with non-advanced Parkinson's disease.

Objectives: To validate [^{18}F]FE-PE2I PET as measurement tool of longitudinal DAT changes in patients with Parkinson's disease.

Methods: Thirty-seven subjects with Parkinson's disease (Hoehn and Yahr stage < 3) were included in a longitudinal PET study with [^{18}F]FE-PE2I. DAT availability (BP_{ND}) in the caudate nucleus, putamen, sensorimotor striatum, and substantia nigra, was estimated with parametric imaging using Logan graphical analysis and cerebellum as reference region. For comparison with DAT-SPECT literature, sample size calculations for disease intervention studies were made.

Results: Baseline and follow-up PET data (interval: 2.3 ± 0.5 years) were available for 25 patients (9 females, 16 males). Median age was 64.7 years (range 46–76); symptom duration: 3 years (0.25–14); Hoehn and Yahr stage (H&Y): 1 (1–2). Annualized DAT decline and effect size were: −8.5 ± 6.6 % and 1.08 for caudate nucleus; −7.1 ± 6.1 % and 1.02 for putamen; −8.3 ± 8.5 % and 0.99 for sensorimotor striatum; −0.11 ± 9.3 % and 0.11 for substantia nigra. The estimated minimum sample size needed for a treatment trial using [^{18}F]FE-PE2I PET as imaging marker is 2–3 times lower than is reported in literature on [^{123}I]FP-CIT SPECT.

Conclusions: Longitudinal [^{18}F]FE-PE2I PET measurements in non-advanced PD demonstrate a striatal DAT decline consistent with previous SPECT and PET studies. No obvious changes of DAT availability were observed in the substantia nigra, indicating perhaps slower progression or compensatory changes. The effect sizes were numerically larger than reported in the literature for other DAT radioligands, suggesting that [^{18}F]FE-PE2I might detect smaller DAT changes, and can be well used as progression marker in clinical trials.

1. Introduction

For decades, molecular imaging of the dopaminergic system in Parkinson's disease (PD) has been used in studies to evaluate the degree of the dopaminergic deficit associated with disease stage, severity, and progression, and as imaging marker in clinical trials. The majority of studies have used the radioligands [^{123}I]β-CIT and [^{123}I]FP-CIT with single photon emission computed tomography (SPECT) (Kaasinen & Vahlberg, 2017), showing good discriminatory power for distinguishing PD from healthy controls (HC), and estimating yearly decline of 6–11 % (Ikeda, Ebina, Kawabe, & Iwasaki, 2019; Kaasinen & Vahlberg, 2017; Li et al., 2018).

In recent years, positron emission tomography (PET) imaging of the dopaminergic system has become more available in the clinical setting due to the wider availability of hybrid PET systems and more established radiochemistry production in research and hospital facilities (Kerstens & Varrone, 2020). The PET radioligand [^{18}F]FE-PE2I was developed at Karolinska Institutet more than a decade ago (Schou, Steiger, Varrone, Guilloteau, & Halldin, 2009) and has been extensively validated in preclinical and clinical studies in healthy controls and patients with

* Corresponding author at: Department of Clinical Neuroscience, BioClinicum J4:14, Visionsgatan 4, 171 64 Solna, Sweden.
E-mail address: Vera.kerstens@ki.se (V.S. Kerstens).

https://doi.org/10.1016/j.nicl.2023.103347
Received 13 October 2022; Received in revised form 7 February 2023; Accepted 10 February 2023
Available online 11 February 2023

Parkinson's disease (Fazio et al., 2018, 2015; Lizana et al., 2018; Sasaki et al., 2012; Schou et al., 2009; Suzuki et al., 2014; Varrone et al., 2011). In non-human primates, the comparison between [^{18}F]FE-PE2I and the similar PET radioligand [^{11}C]PE2I (Varrone et al., 2011) showed that [^{18}F]FE-PE2I had more favourable pharmacokinetic properties and in vivo metabolism. This property was also confirmed in a subsequent healthy human PET study (Fazio et al., 2015). Test-retest studies in healthy controls (Suzuki et al., 2014) and non-advanced PD patients (Kerstens et al., 2020) have shown good reliability and repeatability of [^{18}F]FE-PE2I PET measurements also in small or lower DAT density regions such as the substantia nigra. Recently, [^{18}F]FE-PE2I has also been included in the EANM guideline and SNMMI procedure standard for clinical DAT imaging in Parkinsonian syndromes (Morbelli et al., 2020)).

The preliminary evaluation of an initial cohort of PD patients (n = 12) examined longitudinally with [^{18}F]FE-PE2I PET has already been reported (Brumberg et al., 2021). However, a comprehensive evaluation of the performance of [^{18}F]FE-PE2I PET in measuring longitudinal DAT changes in a better-powered sample size, in sub-regions (including more versus less affected side) of the nigrostriatal system has not been reported yet. Based on a test–retest variability of [^{18}F]FE-PE2I PET measurements up to 10 %, the scan interval of two years was considered to be adequate to measure DAT changes in subjects with non-advanced PD. The study was set up for a sample size of 40 subjects, assuming a drop-out rate of 25 %, based on power calculations using previous findings on DAT.

The aim of this study was to further validate the use of [^{18}F]FE-PE2I PET in non-advanced Parkinson patients. The study was therefore set up: 1) to compare the estimates of DAT decline in PD measured with [^{18}F]FE-PE2I with those previously reported using SPECT and PET radioligands; 2) to calculate the intraindividual effect size of longitudinal DAT changes measured with [^{18}F]FE-PE2I for comparable purposes to the literature; 3) to explore whether DAT changes in patients showing clinical disease progression were larger compared to patients with stable disease; 4) to estimate the minimum sample size needed for clinical trials with disease-modifying interventions using [^{18}F]FE-PE2I PET as imaging marker.

2. Methods

2.1. Ethics

Two studies were combined to enhance sample size and were both approved by the Swedish Ethical Review Authority, the Radiation Safety Committee of the Karolinska University Hospital, and the Swedish Medicinal Product Agency (EudraCT 2011–0020050-30, EudraCT 2017–003327-29 and 2017–001585-19). Patients provided written informed consent for study participation after detailed explanation from the investigator.

2.2. Study population

The study population consists of two consecutive cohorts of patients with non-advanced Parkinson's disease (modified Hoehn and Yahr [H&Y] < 3; Mini Mental Status Exam [MMSE] ≥ 27; age 45–80) that were recruited in separate studies (same principal investigator) and consented to the longitudinal study design with an examination at baseline and after 24 months. **Supplementary Table S1** summarizes the relevant exclusion criteria and rules of conduct to minimize possible confounding factors for DAT measurement. At the time of screening, relevant comorbidities were ruled out through physical examination, basic blood tests, urine drug test, electrocardiography, and structured interview including screening scales for cognitive decline, alcohol dependence, and psychiatric diagnoses.

The first cohort consists of twenty PD patients of which the baseline DAT PET data have already been reported (Fazio et al., 2018). The second cohort consists of twenty PD patients of which the baseline PET of some were part of the previously reported test–retest study (Kerstens et al., 2020).

The relevant differences between the study protocols of the two cohorts consist of 1) the assessment of clinical status in relation to drug treatment ('ON' vs 'OFF', see section 2.3.1), and 2) blood samples collected for GBA gene mutation analysis (L444P, N370S, E326K), which was only done in the second cohort.

2.3. Data collection

2.3.1. Assessment of disease severity and stage

The PD subjects recruited in the first cohort had Unified Parkinson Disease Rating Scale part III (UPDRS-III original version) and H&Y scores assessed during clinical visit while still on their medication ('ON'). These scores were only available for baseline PET. The PD subjects recruited in the second cohort had motor symptom severity assessed with the updated Movement Disorder Society Unified Parkinson Disease Rating Scale part III (MDS-UPDRS-III) and H&Y stage in practically defined 'OFF' state (>12 h off levodopa medication, and > 24 h off dopamine agonists and MAO-B inhibitors), on the day of the PET measurements. For this cohort, these scores were also assessed on the day of the second PET measurement. All other clinical outcome scales used were the same for all subjects. Symptom duration was approximated from the reported onset of motor symptoms.

2.3.2. MRI acquisition

Both T1- and T2-weighted images were acquired with a 3 Tesla MRI system (General Electric, Discovery MR750). The T2-weighted images were used to exclude clinically significant pathology; the T1-weighted images were used for co-registration with the PET images and delineation of the regions of interest (ROI). The T1 sequence had 176 slices of 1 mm thickness, field of view 256 × 256 mm, resolution 1 × 1 × 1 mm, inversion time 450 ms, echo time 3.18 ms, and repetition time 8.16 ms. The same MRI protocol was used for both cohorts.

2.3.3. PET acquisition

The radioligand [^{18}F]FE-PE2I was prepared in-house as previously described (Stepanov et al., 2012). List-mode data were acquired for 93 min following a 6-minute transmission scan with a Caesium-137 source for attenuation correction, as previously described (Fazio et al., 2018, 2015; Kerstens et al., 2020). PET measurements were performed around the same time of day, and in all PD subjects in practically defined 'OFF' state (>12 h off levodopa medication, and > 24 h off dopamine agonists and MAO-B inhibitors).

PET data were reconstructed into 37 frames (8 × 10, 5 × 20, 4 × 30, 4 × 60, 4 × 180, 12 × 360 s) using 3D OP OSEM with 10 iterations and 16 subsets, including modeling of the PSF (Varrone et al., 2009). For both cohorts, data acquisition, and reconstruction were the same.

2.4. Image analysis

In all subjects, PET image analysis was performed as previously reported (Kerstens et al., 2020). In brief, frame-to-frame re-alignment and motion correction was performed using the first two minutes as reference frame for realignment. Motion correction was applied in cases in which a translation of>3 mm was observed in the Z-axis by visual inspection of the realignment plots. Freesurfer was used to automatically delineate striatum, caudate nucleus, putamen, and accumbens area (referred to as ventral striatum in this paper) of both hemispheres. An FSL template was used for automatic delineation of the sensorimotor striatum (https://fsl.fmrib.ox.ac.uk/fsl/fslwiki/Atlases/striatumconn). An in-house developed template was used to automatically delineate the substantia nigra (Fazio et al., 2018). The outcome measure was the binding potential (BP_{ND}), estimated using wavelet-aided parametric imaging (WAPI) (Cselényi, Olsson, Halldin, Gulyás, & Farde, 2006),

with t* = 27 min and using cerebellum as reference region. The more and less affected hemispheres were assigned based on the asymmetry in the putamen BP_{ND} and cross-checked with the asymmetry of the MDS-UPDRS-III score. On a second level, these asymmetry indices were compared with the upper limit of mean 95 % confidence interval of a group of 37 age- and sex-matched healthy control subjects ("HC group 95 % CI") recruited in parallel to the PD cohorts for a separate study (not yet published). Additional reporting was done on only the individual ROIs where asymmetry was above the HC group 95 % CI, to account for non-disease-related measurement variability.

2.5. Data analysis

The data analysis plan was pre-registered at https://aspredicted.org/n3h68.pdf after start of data collection but prior to the start of data analysis.

2.5.1. Statistical analysis

R version 3.6.2 was used for statistical analysis. Shapiro Wilk test was used to assess the normality of distribution; Levene's test for difference in variance between baseline and follow-up variables; and Grubb's test for statistical outliers. Measured percent BP_{ND} change was recalculated per subject to annual percent change, by dividing by the subject's scan interval (yr) using the formula:

[(Follow − up BP_{ND}(ROI))−(baseline BPnd(ROI))] / Baseline BP_{ND}(ROI) * 100/ timediff(yr).

Cohen's dz (Lakens, 2013) was used to assess intraindividual effect size from baseline to follow-up regional BP_{ND}, using the formula: *t-value/* sqrt(*n*). Power was calculated using a significance level of 0.025, one-sample, one-sided *t*-test.

Cohen's ds for interindividual comparisons (Lakens, 2013) was used for the sample size calculations for a clinical trial with a 30 % or 50 % expected treatment effect, using the formula:

(mean expected BP_{ND} decline in placebo group)-(mean expected BP_{ND} decline in treatment group) / pooled SD,

assuming the same SD for the treatment group as for the placebo group.

A priori hypotheses have a p-value threshold of < 0.05 for statistical significance; other comparisons have the threshold adjusted for multiple comparisons with Meff-correction (Derringer, 2018; Li & Ji, 2005) to take into account the high correlation of the ROIs and thus avoid a too conservative correction as would be with the Benjamini Hochberg correction.

2.6. Data sharing

Data is available upon reasonable request.

3. Results

From the original cohorts of patients recruited in the longitudinal studies (n = 40), 9 were excluded and 6 patients were lost at follow-up (see **Supplementary Text** for details). Only one subject had GBA mutation (heterozygote for E326K). The average scan interval was 2.29 ± 0.47 years [interval 1.99–3.78]. The study population is described in Table 1.

3.1. Longitudinal DAT decline and intraindividual effect sizes

The average annual percent decline was estimated to be 5–8.5 % for the striatal regions of interest; the substantia nigra showed no significant decline. The related striatal effect sizes for detection of 2.3 years difference were between 0.81 and 0.97, and for the annualized difference between 0.86 and 1.09. **See Supplementary Table S2 and** Fig. 1. For decline measures of the more versus less affected ROI sides see **Supplementary Table S2 and Supplementary Figure S1.**

A statistically significant exponential DAT decline over symptom duration was observed in caudate nucleus, putamen, and sensorimotor striatum. No evidence of significant DAT decline was seen in the substantia nigra (Fig. 2**,** Table 2 and **Supplementary Figure S2**). See **Supplementary Text** for description of the exponential fitting.

3.2. DAT decline and change in H&Y stage

Because only the second cohort (n = 13) could be used to assess the question of whether change in H&Y stage (assessed in 'OFF') was related to measured DAT change, the analysis was exploratory. Patients who showed an increase (worsening) of ≥ 1H&Y stage between baseline and follow-up PET, had on average higher baseline DAT binding and displayed numerically larger DAT decline than the patients that had the same H&Y stage on both occasions. The difference, however, was not statistically significant (Fig. 3).

3.3. Sample size calculations

The sample size calculations were made for a hypothetical treatment intervention effect with reduced progression of 30 % or 50 % in a two-year clinical trial, using the BP_{ND} of the putamen of the less affected hemisphere or the average BP_{ND} of the putamen of both hemispheres, to match similar calculations in previous literature for comparative purposes. The effect sizes for both regions were similar (Table 3). The minimal sample sizes per group were around 200 subjects in case of a 30 % effect, and around 73 subjects for a 50 % treatment effect (Table 3). Considering an expected drop-out rate of 15 %, the sample size for a two-year treatment study would be between 80 and 240 subjects per group, depending on the region and expected treatment effect.

Table 1
Patient characteristics and clinical data.

	Sex	Age (yr)	Symptom duration (yr)	LEDD (mg)	(MDS-)UPDRS-III	H&Y stage
Baseline						
Total, n = 25	**9F / 16 M**	**64.7 (±7.9) [46–76]**	**3 [0.25–14]**	**342.0 [0–798]**	**–**	**1 [1–2]**
'ON', n = 12	*3F / 9 M*	*60.4 (±7.4) [46–70]*	*2 [0.25–12]*	*270.5 [0–798]*	*19.2 (±7.5) [5–13]*	*1.5 [1–2]*
'OFF', n = 13	*6F / 7 M*	*69.9 [56–76]*	*4.9 (±3.7) [1–14]*	*455 (±199) [111–680]*	*21.2 (±7.4) [10–37]*	*1 [1–2]*
Follow-up				–	–	–
Total, n = 25						
'OFF', n = 13				*613 (±218) [287–1015]*	*22.7 (±9.3) [10–43]*	*2 [1–3]*

Data are summarized as median[range] or mean(±SD) [range] depending on normality of data distribution. Clinical data for the initial cohort that was assessed 'ON' at baseline (n = 12) not systematically re-collected at follow-up. LEDD: levodopa equivalent daily dose. H&Y stage: Hoehn and Yahr stage.

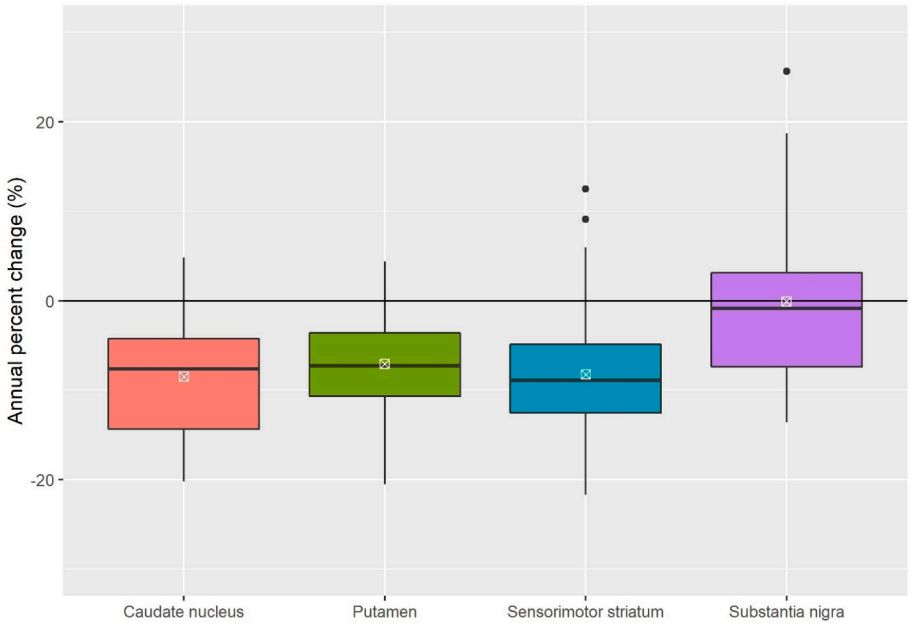

Fig. 1. Boxplot of annual percent change by region of interest. ROI = region of interest.

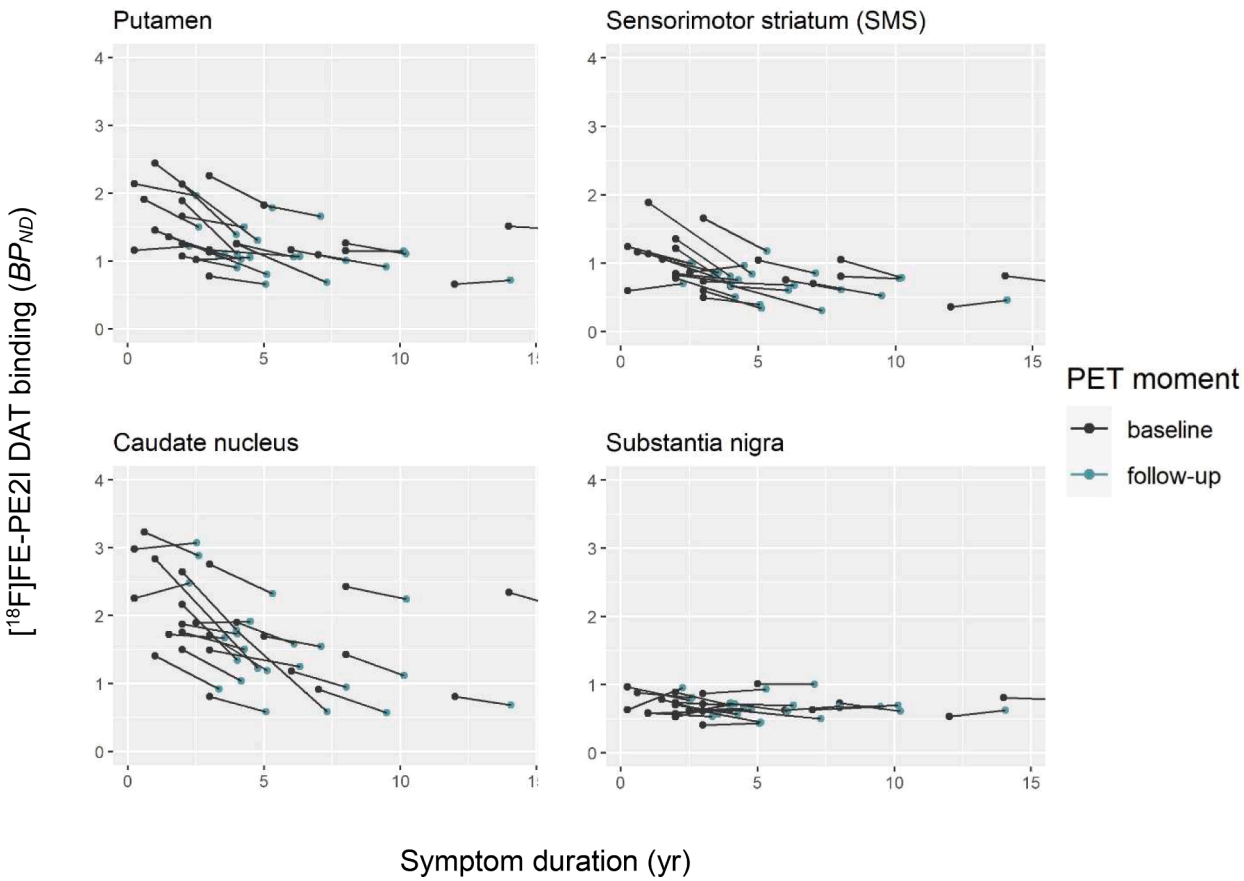

Fig. 2. Individuals' DAT BP_{ND} decline in the putamen, caudate nucleus, sensorimotor striatum, and substantia nigra, are displayed in relation to their respective symptom durations.

Table 2
Exponential regression coefficients of correlation of regional BP_{ND} with symptom duration.

Region	Formula	Residual SE	p-value
Caudate nucleus	$BP_{ND} \sim 2.2 * (SympDur)^{-0.21}$	0.61	0.00004
Putamen	$BP_{ND} \sim 1.57 * (SympDur)^{-0.15}$	0.38	0.00048
Sensorimotor striatum (SMS)	$BP_{ND} \sim 1.00 * (SympDur)^{-0.16}$	0.28	0.0013
Substantia nigra	$BP_{ND} \sim 0.73 * (SympDur)^{-0.04}$	0.14	0.28

4. Discussion

This study was designed to examine the rate of DAT decline measured with [^{18}F]FE-PE2I PET in a group of subjects with non-advanced PD, as part of further validation of [^{18}F]FE-PE2I as imaging marker of nigrostriatal degeneration. To our knowledge, this is the first study to examine longitudinal [^{18}F]FE-PE2I PET measures in a powered cohort of subjects with Parkinson's disease. These data are relevant since [^{18}F]FE-PE2I PET is being used globally by several research groups, as well as implemented in the clinic.

Firstly, we evaluated the consistency of the estimate of annual DAT decline between our data and those previously reported with other SPECT and PET radioligands. Secondly, we calculated the effect size of the DAT change in specific striatal subregions and compared them with those reported for [^{123}I]FP-CIT and [^{11}C]PE2I. Thirdly, we investigated whether the DAT decline was larger in patients with clinical deterioration based on H&Y stage assessment than in patients remaining clinically stable. Finally, we aimed to estimate the minimum sample size needed in a clinical trial to detect a disease-modifying effect of 30 % and 50 % using [^{18}F]FE-PE2I as imaging biomarker, to compare with data available for other DAT radioligands.

4.1. Annual DAT decline

The annual percentage DAT change in striatum of PD's subjects observed in the present study (5–8.5 %) was in agreement with those reported across several previous studies (6–7%) (Chouker et al., 2001; Li et al., 2018; Marek et al., 2002; Staffen, Mair, Unterrainer, Trinka, & Ladurner, 2000; Winogrodzka et al., 2001). The DAT decline observed over symptom duration indicated an exponential decline, which aligns with previous reports of DAT decline over symptom duration (Nandhagopal et al., 2011; Sakakibara et al., 2020).

The data also showed no substantial decline of DAT in the substantia nigra compared to the other regions of the nigrostriatal system. This might indicate a floor effect, compensatory changes in DAT expression, or delayed decline in the disease, consistent with the observation that cell bodies are affected at a later stage of the disease as compared with the nerve terminal (Caminiti et al., 2017; Fazio et al., 2018). The low DAT density in the region and partial volume effect on the small area might have influenced the results as well.

4.2. Intraindividual longitudinal changes and effect sizes

Li and colleagues (Li et al., 2018) performed a similar longitudinal study on 23 subjects with mild-moderate stage PD, using [^{11}C]PE2I PET (scan interval 18.8 months). They found the change of DAT availability

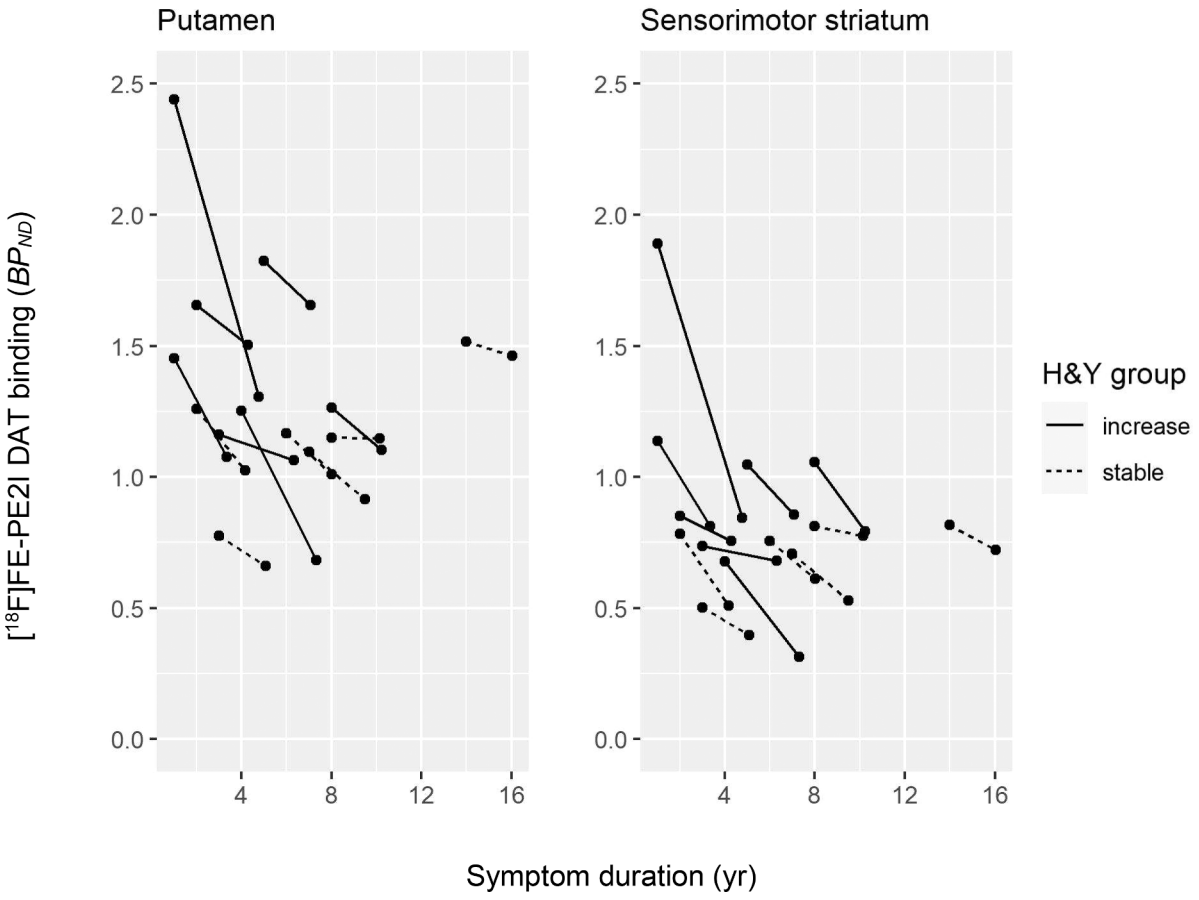

Fig. 3. Individual plots of the relation between DAT binding measured vs symptom duration, categorized by subjects that increased in H&Y stage at follow-up and those that remained the same H&Y stage at follow-up (in the subgroup of cohort with 'OFF'-assessed H&Y stage, n = 13).

Table 3
Sample size calculations using [^{18}F]FE-PE2I BP_{ND} data of the less affected putamen and mean putamen (average of both hemispheres).

	Natural decline DATBP_{ND} (2.3 yr) Mean(SD)	**reatment group decline$_{DAT\ BP_{ND}}$** Mean(SD)	**Effect size** (Cohen's ds)	**Estimated minimal needed sample size per group** [+15 % for drop-outs]
Less affected hemisphere PUTAMEN	−0.408 (0.443)	**30 %:** −0.286 (0.443)	0.28	n = 206 [237]
		50 %: −0.204 (0.443)	0.46	n = 75 [86]
Mean PUTAMEN	−0.272 (0.286)	**30 %:** −0.191 (0.286)	0.29	n = 194 [224]
		50 %: −0.136 (0.286)	0.48	n = 71 [82]

in caudate nucleus and posterior putamen to correlate with the change of total MDS-UPDRS-III score and the bradykinesia-rigidity sub-score, as well as of DAT changes in the more affected putamen with changes of bradykinesia-rigidity score (p =.042). In our study, the sample size of patients with longitudinal MDS-UPDRS-III assessments in 'OFF' (n = 13) was too small to perform a powered correlation analysis. Exploratory analysis did not show any significant correlation between change in DAT and change in MDS-UPDRS-III (sub)scores. However, [^{18}F]FE-PE2I showed a similar pattern of change with MDS-UPDRS-III subscores as [^{11}C]PE2I. See **Supplementary Figure S3**. Therefore, future studies with a higher number of subjects are needed to further assess the correlations.

We also performed an exploratory analysis to evaluate whether the change in H&Y stage was associated with the DAT decline. We observed a trend of larger DAT decline in patients advancing in H&Y stage at follow-up. However, most DAT changes measured were below the minimum detectable difference (measurement variability) (Kerstens et al., 2020). Further studies are needed to explore this association.

The effect size for detecting intraindividual longitudinal DAT change in the putamen measured with [^{18}F]FE-PE2I was about three times larger than those estimated with two- and four-year interval from data of the Parkinson's Progression Markers Initiative (PPMI) cohort examined with [^{123}I]FP-CIT SPECT (Burciu et al., 2017; Marek et al., 2018). This finding would be expected considering the higher sensitivity and resolution of PET vs SPECT which gives the possibility to detect intra-individual differences with higher sensitivity and less variability.

In a previous study conducted in a comparable cohort of 23 non-advanced PD subjects that were examined with [^{11}C]PE2I PET with a 18.8-month interval (Li et al., 2018), the estimated intraindividual effect size was around 0.71–0.78 for the caudate nucleus, posterior and anterior putamen. With our data recalculated to 18.8 months, the effect sizes of caudate nucleus and putamen are 1.02—1.08. The difference between the effect sizes calculated from BP_{ND} values obtained with [^{18}F]FE-PE2I and those obtained with [^{11}C]PE2I might be related to differences in the methods of image analysis or differences in the resolution of the PET systems used in the two studies. [^{18}F]FE-PE2I, however, has some advantages over [^{11}C]PE2I. Due to the longer half-life of ^{18}F vs ^{11}C, [^{18}F]FE-PE2I can be distributed also to centres that do not have a radioligand-production facility. Furthermore, the fast kinetic properties of [^{18}F]FE-PE2I and the low production of blood–brain barrier crossing radiometabolites are also advantages in terms of quantification (Fazio et al., 2015; Kukk, Loog, Hiltunen, & Järv, 2018; Morbelli et al., 2020; Sasaki et al., 2012; Varrone et al., 2009; Varrone et al., 2011).

4.3. Sample size calculation

The sample size calculation with the data obtained with [^{18}F]FE-PE2I PET and those reported in previous [^{123}I]FP-CIT SPECT studies (Burciu et al., 2017; Marek et al., 2018), showed that for a 2.3-year randomized clinical trial with a 50 % effect (power = 0.8, a two-sided alpha = 0.05) the number of participants needed using [^{18}F]FE-PE2I PET would be 2–3 times lower than the number of participants needed for a 2-year trial using [^{123}I]FP-CIT SPECT (80 vs 168 to 236). No data is available on other current DAT radioligands' sample size calculations assuming a 30 % treatment effect (which perhaps would be more realistic), but one assumes a similar comparative advantage of sample needed using [^{18}F]FE-PE2I. The amount of PET facilities using [^{18}F]FE-PE2I is growing globally over the past years and has been implemented in a few clinics, providing the possibility for multi-center collaborative studies to reach the powered sample sizes. To enable implementation across sites, such studies would benefit from simplified quantification methods with short acquisition protocols (e.g. 30-minute early SBR as in Brumberg et al., 2021). In such case, it is expected that the needed sample size would be larger than the one reported in this study.

Calculating sample size on *non-advanced* Parkinson patients is relevant because this population is likely to have a measurable decline in DAT and, additionally, is the likely target group for disease-modifying treatments.

4.4. Genetic and pharmacological factors

One subject from the second cohort was found to be heterozygote of a GBA mutation (E326K). E326K mutations are associated with marginally earlier disease onset and a higher prevalence of cognitive decline (O'Regan, Desouza, Balestrino, & Schapira, 2017) – which was not the case in this subject.

Although there is no strong evidence of the possible neuroprotective or neurotoxic effect of anti-Parkinson medication, we acknowledge that this potential confounding factor could not be excluded in the present study. However, since estimates of DAT decline were similar to those reported in previous studies in different cohorts, including unmedicated patients, we believe that our study cohort reflects a representative group of PD patients.

Finally, two subjects mentioned the COVID-19 pandemic significantly influenced their physical training routine which influenced their experienced severity of motor symptoms, reflected in the MDS-UPDRS-III score.

4.5. Outlier subject

One of the subjects that completed the study was excluded from the final report (described in the Supplementary Text) because no unbiased decision could be made on which of its baseline PETs to take as baseline. This subject had two baseline PETs as they were also part of our test–retest study (Kerstens et al., 2020), and showed an unexpectedly high test–retest DAT BP_{ND} variability, unexplained by external factors. For the sake of transparency, we report in Supplementary Table S3 the results including this subject with either PET as baseline. Overall, the same conclusions can be made regarding the validity of measuring DAT with [^{18}F]FE-PE2I PET, its comparisons to other DAT radioligand reports in the literature, and a 2–2,5 times lower sample size needed than reported in the literature on FP-CIT SPECT.

5. Conclusions

The present study shows that [^{18}F]FE-PE2I PET is able to measure longitudinal DAT changes in patients with non-advanced Parkinson's disease with larger effect sizes compared with other DAT SPECT and PET radioligands. It thereby proves to be a beneficial disease progression marker. Considering the sample size calculations and the known advantages of PET vs SPECT, [^{18}F]FE-PE2I can be considered as a potential imaging marker in future clinical trials with disease-modifying interventions.

Declaration of Competing Interest

The authors declare that they have no known competing financial interests or personal relationships that could have appeared to influence the work reported in this paper.

Data availability

Data will be made available on request.

Acknowledgements

The authors would like to thank Malena Kjellén and Karin Lycke for the help with data collection, and Zsolt Cselényi for the development of an automated PET analysis software.

Financial disclosure/conflict of interest

At the time of writing of the manuscript, Andrea Varrone is employed at H. Lundbeck A/S.

Funding Sources for study

Swedish science council, Åhlen Foundation, H Lundbeck A/S, and a private donation.

Appendix A. Supplementary data

Supplementary data to this article can be found online at https://doi.org/10.1016/j.nicl.2023.103347.

References

Brumberg, J., Kerstens, V., Cselényi, Z., Svenningsson, P., Sundgren, M., Fazio, P., Varrone, A., 2021. Simplified quantification of [18F]FE-PE2I PET in Parkinson's disease: Discriminative power, test–retest reliability and longitudinal validity during early peak and late pseudo-equilibrium. Journal of Cerebral Blood Flow and Metabolism 41 (6), 1291–1300. https://doi.org/10.1177/0271678X20958755.

Burciu, R. G., Ofori, E., Archer, D. B., Wu, S. S., Pasternak, O., McFarland, N. R., … Vaillancourt, D. E. (2017). Progression marker of Parkinson's disease: a 4-year multi-site imaging study. *Brain*, *140*(8), 2183–2192. https://doi.org/10.1093/BRAIN/AWX146.

Caminiti, S.P., Presotto, L., Baroncini, D., Garibotto, V., Moresco, R.M., Gianolli, L., Volonté, M.A., Antonini, A., Perani, D., 2017. Axonal damage and loss of connectivity in nigrostriatal and mesolimbic dopamine pathways in early Parkinson's disease. NeuroImage. Clinical 14, 734–740.

Chouker, M., Tatsch, K., Linke, R., Pogarell, O., Hahn, K., Schwarz, J., 2001. Striatal dopamine transporter binding in early to moderately advanced parkinson's disease: Monitoring of disease progression over 2 years. Nuclear Medicine Communications 22 (6), 721–725. https://doi.org/10.1097/00006231-200106000-00017.

Cselényi, Z., Olsson, H., Halldin, C., Gulyás, B., Farde, L., 2006. A comparison of recent parametric neuroreceptor mapping approaches based on measurements with the high affinity PET radioligands [11C]FLB 457 and [11C]WAY 100635. NeuroImage. 32 (4), 1690–1708. https://doi.org/10.1016/j.neuroimage.2006.02.053.

Derringer, J. (2018). A simple correction for non-independent tests. https://doi.org/10.31234/OSF.IO/F2TYW.

Fazio, P., Svenningsson, P., Forsberg, A., Jönsson, E.G., Amini, N., Nakao, R., Nag, S., Halldin, C., Farde, L., Varrone, A., 2015. Quantitative Analysis of ^{18}F-(E)-N-(3-Iodoprop-2-Enyl)-2β-Carbofluoroethoxy-3β-(4'-Methyl-Phenyl) Nortropane Binding to the Dopamine Transporter in Parkinson Disease. Journal of Nuclear Medicine : Official Publication, Society of Nuclear Medicine 56 (5), 714–720.

Fazio, P., Svenningsson, P., Cselényi, Z., Halldin, C., Farde, L., Varrone, A., 2018. Nigrostriatal dopamine transporter availability in early Parkinson's disease. Movement Disorders 33 (4), 592–599. https://doi.org/10.1002/mds.27316.

Ikeda, K., Ebina, J., Kawabe, K., Iwasaki, Y., 2019. Dopamine transporter imaging in parkinson disease: Progressive changes and therapeutic modification after anti-parkinsonian medications. Internal Medicine. 58 (12), 1665–1672. https://doi.org/10.2169/internalmedicine.2489-18.

Kaasinen, V., Vahlberg, T., 2017. Striatal dopamine in Parkinson disease: A meta-analysis of imaging studies. Annals of Neurology. 82 (6), 873–882. https://doi.org/10.1002/ana.25103.

Kerstens, V.S., Fazio, P., Sundgren, M., Matheson, G.J., Franzén, E., Halldin, C., Cervenka, S., Svenningsson, P., Varrone, A., 2020. Reliability of dopamine transporter PET measurements with [18F]FE-PE2I in patients with Parkinson's disease. EJNMMI Research 10 (1). https://doi.org/10.1186/s13550-020-00676-4.

Kerstens, V.S., Varrone, A., 2020. Dopamine transporter imaging in neurodegenerative movement disorders: PET vs. SPECT. *Clinical and Translational Imaging* 8 (5), 349–356. https://doi.org/10.1007/s40336-020-00386-w.

Kukk, S., Loog, O., Hiltunen, J.V., Järv, J., 2018. In Vitro Ligand Binding Kinetics Explains the Pharmacokinetics of [18 F]FE-PE2I in Dopamine Transporter PET Imaging. ACS Medicinal Chemistry Letters. 9 (12), 1292–1296. https://doi.org/10.1021/acsmedchemlett.8b00504.

Lakens, D., 2013. Calculating and reporting effect sizes to facilitate cumulative science: A practical primer for t-tests and ANOVAs. Frontiers in Psychology 4 (NOV), 863. https://doi.org/10.3389/FPSYG.2013.00863/ABSTRACT.

Li, J., Ji, L., 2005. Adjusting multiple testing in multilocus analyses using the eigenvalues of a correlation matrix. Heredity 95 (3), 221–227.

Li, W., Lao-Kaim, N.P., Roussakis, A.A., Martín-Bastida, A., Valle-Guzman, N., Paul, G., Loane, C., Widner, H., Politis, M., Foltynie, T., Barker, R.A., Piccini, P., 2018. 11C-PE2I and 18F-Dopa PET for assessing progression rate in Parkinson's: A longitudinal study. Movement Disorders. 33 (1), 117–127.

Lizana, H., Johansson, L., Axelsson, J., Larsson, A., Ögren, M., Linder, J., Halldin, C., Varrone, A., Mo, S.J., 2018. Whole-body biodistribution and dosimetry of the dopamine transporter Radioligand 18 F-FE-PE2I in human subjects. Journal of Nuclear Medicine 59 (8), 1275–1280.

Marek, K, Seibyl, J., Caspell-Garcia, C., Coffey, C., Mollenhauer, B., Kieburtz, K., … Simuni, T. (2018). PPMI driven sample size estimation for clinical trials in Parkinson's disease. Retrieved February 9, 2022, from https://www.mdsabstracts.org/abstract/ppmi-driven-sample-size-estimation-for-clinical-trials-in-parkinsons-disease/%0Ahttp://ovidsp.ovid.com/ovidweb.cgi?T=JS&CSC=Y&NEWS=N&PAGE=fulltext&D=emed19&AN=624550616 https://ucl-new-primo.hosted.exlibrisgroup.c.

Marek, K., Seibyl, J., Shoulson, I., Holloway, R., Kieburtz, K., McDermott, M., Welsh, M., 2002. Dopamine Transporter Brain Imaging to Assess the Effects of Pramipexole vs Levodopa on Parkinson Disease Progression. JAMA 287 (13), 1653–1661. https://doi.org/10.1001/JAMA.287.13.1653.

Morbelli, S., Esposito, G., Arbizu, J., Barthel, H., Boellaard, R., Bohnen, N.I., Brooks, D.J., Darcourt, J., Dickson, J.C., Douglas, D., Drzezga, A., Dubroff, J., Ekmekcioglu, O., Garibotto, V., Herscovitch, P., Kuo, P., Lammertsma, A., Pappata, S., Peñuelas, I., Seibyl, J., Semah, F., Tossici-Bolt, L., Van de Giessen, E., Van Laere, K., Varrone, A., Wanner, M., Zubal, G., Law, I., 2020. EANM practice guideline/SNMMI procedure standard for dopaminergic imaging in Parkinsonian syndromes 1.0. European Journal of Nuclear Medicine and Molecular Imaging 47 (8), 1885–1912.

Nandhagopal, R., Kuramoto, L., Schulzer, M., Mak, E., Cragg, J., McKenzie, J., … Stoessl, A. J. (2011). Longitudinal evolution of compensatory changes in striatal dopamine processing in Parkinson's disease. *Brain*. 134(Pt 11):3290-8. https://doi.org/10.1093/brain/awr233.

O'Regan, G., Desouza, R.M., Balestrino, R., Schapira, A.H., 2017. Glucocerebrosidase Mutations in Parkinson Disease. Journal of Parkinson's Disease. 7 (3), 411–422. https://doi.org/10.3233/JPD-171092.

Sakakibara, S., Hashimoto, R., Katayama, T., Kenjyo, M., Yokokawa, Y., Saito, Y., Hirakawa, A., Ito, M., Nakamura, T., Hara, K., Hashizume, A., Aiba, I., Inukai, A., Katsuno, M., 2020. Longitudinal Change of DAT SPECT in Parkinson's Disease and Multiple System Atrophy. Journal of Parkinson's Disease 10 (1), 123–130.

Sasaki, T., Ito, H., Kimura, Y., Arakawa, R., Takano, H., Seki, C., Kodaka, F., Fujie, S., Takahata, K., Nogami, T., Suzuki, M., Fujiwara, H., Takahashi, H., Nakao, R., Fukumura, T., Varrone, A., Halldin, C., Nishikawa, T., Suhara, T., 2012. Quantification of dopamine transporter in human brain using PET with 18F-FE-PE2I. Journal of Nuclear Medicine : Official Publication, Society of Nuclear Medicine 53 (7), 1065–1073.

Schou, M., Steiger, C., Varrone, A., Guilloteau, D., Halldin, C., 2009. Synthesis, radiolabeling and preliminary in vivo evaluation of [18F]FE-PE2I, a new probe for the dopamine transporter. Bioorganic and Medicinal Chemistry Letters. 19 (16), 4843–4845. https://doi.org/10.1016/j.bmcl.2009.06.032.

Staffen, W., Mair, A., Unterrainer, J., Trinka, E., Ladurner, G., 2000. Measuring the progression of idiopathic Parkinson's disease with [123I] β-CIT SPECT. Journal of Neural Transmission 107 (5), 543–552. https://doi.org/10.1007/s007020070077.

Stepanov, V., Krasikova, R., Raus, L., Loog, O., Hiltunen, J., Halldin, C., 2012. An efficient one-step radiosynthesis of [18F]FE-PE2I, a PET radioligand for imaging of dopamine transporters. Journal of Labelled Compounds and Radiopharmaceuticals 55 (6), 206–210. https://doi.org/10.1002/jlcr.2927.

Suzuki, M., Ito, H., Kodaka, F., Takano, H., Kimura, Y., Fujiwara, H., To, C., 2014. Reproducibility of PET measurement for presynaptic dopaminergic functions using L-[b- 11 C]DOPA and [18 F]FE-PE2I in humans. Nucl Med Commun Wolters Kluwer Health. Nuclear Medicine Communications 35 (35). https://doi.org/10.1097/MNM.0000000000000052.

Varrone, A., Sjöholm, N., Eriksson, L., Gulyás, B., Halldin, C., Farde, L., 2009. Advancement in PET quantification using 3D-OP-OSEM point spread function reconstruction with the HRRT. European Journal of Nuclear Medicine and Molecular Imaging 36 (10), 1639–1650. https://doi.org/10.1007/s00259-009-1156-3.

Varrone, A., Tóth, M., Steiger, C., Takano, A., Guilloteau, D., Ichise, M., Gulyás, B., Halldin, C., 2011. Kinetic analysis and quantification of the dopamine transporter in the nonhuman primate brain with 11C-PE2I and 18F-FE-PE2I. Journal of Nuclear Medicine. 52 (1), 132–139.

Winogrodzka, A., Bergmans, P., Booij, J., van Royen, E.A., Janssen, A.G., Wolters, E.C., 2001. [123I]FP-CIT SPECT is a useful method to monitor the rate of dopaminergic degeneration in early-stage Parkinson's disease. J Neural Transm. 108 (8–9), 1011–1019. https://doi.org/10.1007/s007020170019.